REMARKS

Claims 1, 4, 5 and 12 have been amended to recite that the lithium transition metal complex oxide containing Ni and Mn as transition metals, having a layered structure, and containing fluorine, of the battery and method of the present invention is obtained by heat treating a mixture of a fluorine compound and raw materials used to formulate the lithium transition metal complex oxide. This amendment is supported in the specification by the description at page 22, line 25, to page 23, line 4.

Referring to the Final Action, claims 1, 4-9, 12 [sic], 14-21 and 24-29 are rejected under 35 U.S.C. § 103(a) as being unpatentable over Kazuhara (JP 2002-100357) in view of Yamaura (JP 08-213014). Claim 3 is rejected under 35 U.S.C. § 103(a) as being unpatentable over Kazuhara in view of Yamaura and further in view of Goto, U.S. Patent No. 6,444,351.

Kazuhara is alleged in the rejection to disclose a nonaqueous electrolyte secondary battery containing each of the limitations of the rejected claims including a lithium transition metal complex oxide and lithium cobaltate as the positive electrode material, the lithium transition metal complex oxide containing Ni and Mn as transition metals and having a layered structure except, however, that the lithium transition metal complex oxide of Kazuhara does

not contain fluorine. Yamaura is cited as teaching the application of a fluorination treatment to a lithium transition metal composite oxide composite.

The conclusion of the Office is that it would have been obvious to fluorinate the positive active material of Kazuhara according to the teachings of Yamaura.

In the amendment filed October 27, 2008, to the Office Action dated June 26, 2008, in response to the same rejection of the claims, applicants explained that the proposed modification of Kazuhara according to the teachings of Yamaura, alone or in combination with Goto, would not have resulted in the nonaqueous electrolyte secondary battery of the present invention.

The proposed modification of Kazuhara according to the teachings of Yamaura would not have resulted in the nonaqueous electrolyte secondary battery of the present invention because Yamaura discloses a fluorination treatment of a lithium transition metal composite oxide particle that is conducted with a fluorine compound represented by, for example, $R_1R_2R_3R_4NF$. As shown in Fig. 1 and described in paragraph [0030] of Yamaura, the fluorination treatment results in OH groups on the surface of the lithium transition metal complex oxide particle being replaced with fluorine atoms.

In the present invention, on the other hand, as defined in the claims, the lithium transition metal complex oxide is obtained by heat treating a mixture of a fluorine compound and raw materials used to formulate the lithium transition metal complex oxide and, as a result of the heat treatment of the mixture, fluorine exists inside the lithium transition metal complex oxide - not only at the surface.

In the Final Action, the Office takes the position that the fluorinated transition metal oxide structure of the prior art is similar to the applicants' because "mixing the raw material of the Applicant's Mn0.33Ni0.33Co0.34(OH)2 with fluorine is *close* to mixing the final product LiMn0.33Ni0.33Co0.34(OH)2 ...". (Action, page 4, lines 11-13). (Emphasis applicants'). The Office cites *In re Marosi*, 710 F.2d 798, 802, 218 USPQ 289, 292 (Fed. Cir. 1983) as supporting its position regarding the "obviousness" of the lithium transition metal complex oxide.

In order to rebut the position of the Office regarding any apparent identity or similarity of the lithium transition metal complex oxide containing fluorine of the battery of the present invention to the fluorinated transition metal oxide of Yamaura, applicants, as noted above, have amended the claims of the application to recite that the lithium transition metal complex

oxide containing fluorine is obtained by heat treating a mixture of a fluorine compound and raw materials used to formulate the lithium transition metal complex oxide. Yamaura, on the other hand, discloses only a fluorination treatment of a lithium transition metal composite oxide particle that is conducted with a fluorine compound represented by, for example, $R_1R_2R_3R_4NF$; or by reacting the particle directly with F_2 gas, contacting the particle with NF_3 gas, using AHF (Anhydrous Hydrogen Fluoride), or photochemically fluorinating the particle using a perfluorocompound. Yamaura does not disclose heat treating a mixture of a fluorine compound and raw materials of a lithium transition metal complex oxide.

Additionally, submitted herewith as evidence showing that the fluorine exists inside the complex oxide in the present invention is a copy of G.-H. Kim et al., *Journal of The Electrochemical Society*, 152 (9) A1707 - A1713 (2005). In the Kim et al. publication, a complex oxide is prepared by substantially the same process as in Example 4 of the present specification (see page A1707, right column, lines 2 - 3) and as recited in the claims of the present application. The publication discloses that "XRD results clearly confirm that fluorine ions are successfully substituted for oxygen ions in Li[Ni1/3Co1/3Mn1/3]O2 structure". (Page A1709, left column, lines 19 - 21). (Emphasis applicants').

The Kim et al. publication also describes that in order to study the distribution of fluorine "within a particle", X-ray photoelectron spectroscopy (XPS) analysis of $Li[Ni_{1/3}Co_{1/3}Mn_{1/3}]O_{1.95}F_{0.5}$ was carried out (page A1709, right column, lines 1-4 of the paragraph beginning in the middle of the page). The publication concludes that "XPS analysis also shows the majority of the fluorine ions reside near the surface of the particle. These results suggest that fluorine ions are both in bulk and on the surface of $Li[Ni_{1/3}Co_{1/3}Mn_{1/3}]O_{2-z}F_z$". (Page A1712, right column, lines 9 - 12). As used in the publication, the term "the surface" in the phrase "on the surface of $Li[Ni_{1/3}Co_{1/3}Mn_{1/3}]O_{2-z}F_z$" means the bulk portion near the surface, not the outermost surface. (See the sentence bridging pages A1709 and A1710 of the publication which describes "XRD and XPS analysis clearly demonstrated that fluorine resides in the bulk as well as near the surface of the particle"). (Emphasis applicants').

In contrast, in Yamaura, OH groups only at the outermost surface are replaced with fluorine as shown in Fig. 1 of Yamaura. (Yamaura describes (paragraph [0028]) that oxygen in the outermost surface layer of the lithium transition metal complex oxide particle reacts nucleophilically with a solvent to form a weak bond with hydrogen. Therefore, oxygen in the outermost layer of the

lithium transition metal complex oxide particle bonds with hydrogen from the outside to form the OH group. Accordingly, the OH group is not part of the crystal structure of the lithium transition metal complex oxide and the fluorine that replaces the OH groups exists only at the outermost surface layer of the lithium transition metal complex oxide particle).

The Kim et al. publication establishes the "unobvious difference" between the product of Yamaura and that of the present invention as required by *Marosi* and demonstrates the unobviousness of the claims of the present application over the combination of Kazuhara and Yamaura.

Removal of the 35 U.S.C. § 103(a) rejections of the claims based on Kazuhara in view of Yamaura and based on Kazuhara in view of Yamaura and further in view of Goto is in order.

Claims 1, 4-9, 12 [sic], 14-21 and 24-29 are also rejected under 35 U.S.C. § 103(a) as being unpatentable over Kazuhara in view of Nishida (EP 1246279). Claim 3 is rejected under 35 U.S.C. § 103(a) as being unpatentable over Kazuhara in view of Nishida and further in view of Goto.

Applicants respectfully submit that the proposed modification of Kazuhara according to the teachings of Nishida will not result in the battery of the present invention.

The insufficiencies of Kazuhara are discussed above. Nishida discloses only halogenation of lithium containing cobalt composite oxide, not lithium-nickel-manganese complex oxide. Therefore, if the teachings of Nishida are applied to the positive active material of Kazuhara, lithium-cobalt complex oxide is halogenated, while lithium-nickel-manganese complex oxide is not halogenated. According to the present invention, lithium-nickel-manganese complex oxide should be fluorinated, because lithium-nickel-manganese complex oxide shows a very large battery expansion, as shown in Table 5 of the present specification. Please note the description on page 10, line 23, to page 11, line 7, of the present specification.

Removal of the 35 U.S.C. § 103(a) rejections of the claims based on Kazuhara in view of Nishida and based on Kazuhara in view of Nishida and further in view of Goto is also in order.

The foregoing is believed to be a complete and proper response to the Final Office Action dated May 14, 2009, and is believed to place this application in condition for allowance.

In the event that this paper is not considered to be timely filed, applicants hereby petition for an appropriate extension of time. The fee for any such extension may be charged to Deposit Account No. 111833.

PATENT APPLN. NO. 10/522,771 **PATENT**
SUBMISSION UNDER 37 C.F.R. § 1.114

In the event any additional fees are required, please also charge Deposit Account No. 111833.

Respectfully submitted,
KUBOVCIK & KUBOVCIK

Ronald J. Kubovcik
Reg. No. 25,401

Crystal Gateway 3
Suite 1105
1215 South Clark Street
Arlington, VA 22202
Tel: (703) 412-9494
Fax: (703) 412-9345
RJK/ff

Journal of The Electrochemical Society, 152 (9) A1707-A1713 (2005)
0013-4651/2005/152(9)/A1707/7/$7.00 © The Electrochemical Society, Inc.

Improvement of High-Voltage Cycling Behavior of Surface-Modified $Li[Ni_{1/3}Co_{1/3}Mn_{1/3}]O_2$ Cathodes by Fluorine Substitution for Li-Ion Batteries

G.-H. Kim,[a] J.-H. Kim,[a] S.-T. Myung,[b,*] C. S. Yoon,[a] and Y.-K. Sun[a,*,z]

[a]Department of Chemical Engineering, Center for Information and Communication Materials, Hanyang University, Seoul 133-791, Korea
[b]VK Corporation, Pyongtaek-City, Kyonggi-do 450-090, Korea

To improve the electrochemical property of $Li[Ni_{1/3}Co_{1/3}Mn_{1/3}]O_2$ at high upper voltage limit of 4.6 V, fluorine was partly substituted for oxygen. Variation of lattice parameters and X-ray photoelectron spectroscopy analysis suggest that fluorine is both substituted in bulk and coated on the surface of $Li[Ni_{1/3}Co_{1/3}Mn_{1/3}]O_2$. $Li[Ni_{1/3}Co_{1/3}Mn_{1/3}]O_{2-z}F_z$ ($z = 0.05$ and 0.1) showed stable cycling performance and improvement of high rate capability compared to bare $Li[Ni_{1/3}Co_{1/3}Mn_{1/3}]O_2$. In addition, fluorine substitution catalyzes the growth of the primary particles, which in turn resulted in high tap density as well as high volumetric capacity compared to $Li[Ni_{1/3}Co_{1/3}Mn_{1/3}]O_2$. Differential scanning calorimetry at 4.6 V clearly shows that fluorine substitution markedly improves the thermal stability of $Li[Ni_{1/3}Co_{1/3}Mn_{1/3}]O_{2-z}F_z$.

Manuscript submitted January 5, 2005; revised manuscript received March 21, 2005. Available electronically July 21, 2005.

During the past decade, the lithium transition-metal oxides, $Li[Ni_zCo_{1-2z}Mn_z]O_2$, have received a great deal of interest as a cathode material for Li-ion secondary batteries.[1-3] Among them, $Li[Ni_{1/3}Co_{1/3}Mn_{1/3}]O_2$ has been studied extensively as a promising cathode material for lithium secondary batteries. In attempts to increase the reversible capacity of the cathode material, the upper cutoff voltage limit has been gradually increased. The increased upper voltage limit resulted in a moderate increase in the specific discharge capacity as expected. However, the improved discharge capacity was accompanied by unstable cycling performance when cycled up to 4.6 V.[4,5] Moreover, even at upper voltage limits of 4.4–4.5 V, capacity fading was still observed upon cycling. The origin of this capacity fading was mainly attributed to gradual decaying of electroactive Co as reported by Shaju et al.[4]

$LiCoO_2$, a commercialized cathode material, also has shown poor electrochemical properties when the upper voltage limits were higher than 4.2 V because of its phase transition from hexagonal to monoclinic. Moreover, it has been reported that the poor electrochemical properties of $LiCoO_2$ at high voltage are due to the dissolution of Co ions into electrolyte[6]. To solve this problem, various metal oxides were coated onto or substituted for $LiCoO_2$.[7-15] It was proposed that the metal oxide coating or substitution effectively reduced the Co dissolution, which accordingly led to the improvement in capacity retention at the high-voltage region.[16,17] Among them, 10% of Al-doped $LiAl_yCo_{1-y}O_2$ had less electrolyte decomposition with good electrochemical performances. Also, the use of aluminum ions as a dopant in transition-metal layered structure has a beneficial effect on suppressing the anisotropic structural change, because the Al^{3+} ions together with lithium ions kept the interlayer distance during delithiation.[18] In addition, anion substitution for O has been also studied in $LiCoO_2$ coated with fluorine, which substantially suppressed the Co dissolution even at the high upper voltage limit of 4.3 V.[19]

To suppress Co dissolution, and thereby to improve the electrochemical property at the high-voltage region, we substituted fluorine for oxygen in the $Li[Ni_{1/3}Co_{1/3}Mn_{1/3}]O_2$. In this paper, we report the effects of fluorine substitution on the structure, electrochemical behavior, and thermal stability of $Li[Ni_{1/3}Co_{1/3}Mn_{1/3}]O_{2-z}F_z$ (where $0 < z < 0.5$).

Experimental

$LiOH \cdot H_2O$, $CoSO_4 \cdot 7H_2O$, $NiSO_4 \cdot 6H_2O$, and $MnSO_4 \cdot H_2O$ were used as starting materials. $[Ni_{1/3}Co_{1/3}Mn_{1/3}](OH)_x$ compounds were synthesized by the coprecipitation method, as reported previously.[20] A mixture of the dehydrated $[Ni_{1/3}Co_{1/3}Mn_{1/3}](OH)_x$ and $LiOH \cdot H_2O$ and LiF was heated at 1000°C for 10 h, then subsequently annealed at 700°C for 5 h in air atmosphere. An excess of lithium was used to compensate for lithium loss during the calcination. Chemical compositions of the resulting powders were analyzed by atomic absorption spectroscopy (Vario 6, Analytikjena) and ion chromatography (DX-320, Dionex, USA) for fluorine.

Powder X-ray diffraction (XRD, Rint-2000, Rigaku, Japan) measurement using Cu Kα radiation was employed to identify the crystalline phase of the synthesized materials. XRD data were obtained $2\theta = 10$–$80°$ with a step size of 0.03° and a count time of 5 s. From the XRD data, lattice parameters of $Li[Ni_{1/3}Co_{1/3}Mn_{1/3}]O_{2-z}F_z$ were calculated by the least-squares method. The morphology of as-prepared powders was observed using a scanning electron microscope (SEM, JSM 6400, JEOL, Japan).

Pellet density (PD) of the oxides was obtained by making 8 mm diam pellets with approximately 500 mg powder under a pressure of

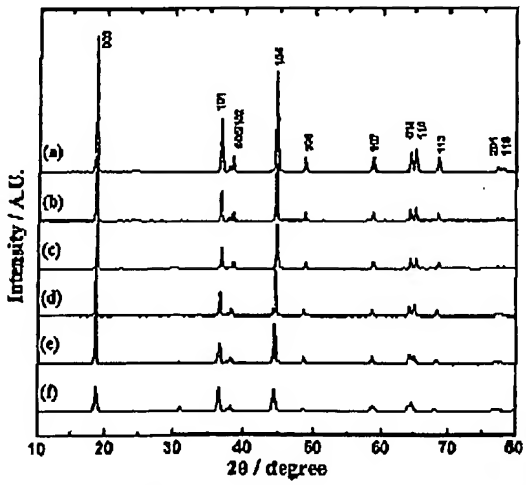

Figure 1. Powder XRD profiles of $Li[Ni_{1/3}Co_{1/3}Mn_{1/3}]O_{2-z}F_z$: (a) $z = 0$, (b) $z = 0.05$, (c) $z = 0.1$, (d) $z = 0.15$, (e) $z = 0.2$, and (f) $z = 0.5$.

* Electrochemical Society Active Member.
z E-mail: yksun@hanyang.ac.kr

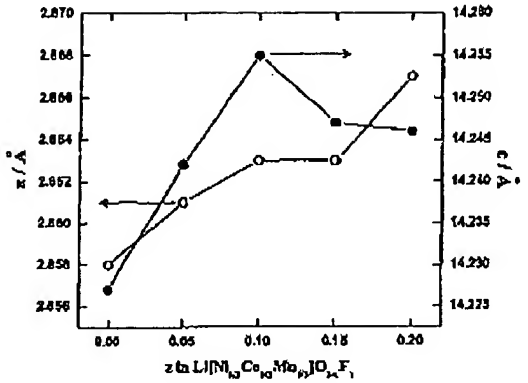

Figure 2. Variation of lattice parameters a and c as a function of F content in $Li[Ni_{1/3}Co_{1/3}Mn_{1/3}]O_{2-z}F_z$.

48,000 psi. The thickness and diameter of the pellet after pressing was measured and the density was then calculated. The error is estimated to be ±0.08 g/cm³.

The cathode was prepared by blending $Li[Ni_{1/3}Co_{1/3}Mn_{1/3}]O_{2-z}F_z$, Super S carbon black, and polyvinylidene fluoride (80:10:10 in weight ratio) in *N*-methyl-2-pyrrolidone. The slurry was then cast on an aluminum foil and dried at 110°C overnight in vacuum state. Disks were then punched out of the foil. Lithium foil was used as an anode. The long cycle-life tests were performed by employing mesocarbon microbead analysis (MCMB) as an anode. Cell tests were done using a 2032 coin-type cell. The electrolyte solution was 1 M $LiPF_6$ in a mixture of ethylene carbonate (EC) and diethyl carbonate (DEC) in a 1:1 volume ratio. Then the coin-type cell was assembled in an argon-filled dry box and tested at a current density of 28 mA g^{-1} (0.2 C) at 30°C.

For differential scanning calorimetry (DSC) experiments, the cells were fully charged to 4.6 V and opened in the Ar-filled dry box. After the remaining electrolyte was carefully removed from the surface of the electrode, the cathode materials were recovered from the current collector. A stainless steel sealed pan with a gold-plated copper seal (which can withstand 150 atm of pressure before rupturing and has a capacity of 30 μL) was used to collect 3–5 mg samples. The recovered composite cathode was infiltrated with about 0.5 mg of electrolyte. The measurements were carried out in a DSC 200 differential scanning calorimeter (NETZSH, Germany) using a temperature scan rate of 1°C min^{-1}. The weight of each sample (pan + sample) was measured before and after the experiment to verify that the system was hermetically sealed. The weight was constant in all cases, indicating that there were no leaks during the experiments.

Results and Discussion

XRD analysis of $Li[Ni_{1/3}Co_{1/3}Mn_{1/3}]O_{2-z}F_z$.—Figure 1 shows XRD patterns of $Li[Ni_{1/3}Co_{1/3}Mn_{1/3}]O_{2-z}F_z$ with $z = 0$, 0.05, 0.1, 0.15, 0.2, and 0.5. The XRD patterns could be indexed by a hexagonal α-$NaFeO_2$ structure (space group $R\bar{3}m$). The $Li[Ni_{1/3}Co_{1/3}Mn_{1/3}]O_{2-z}F_z$ shows clear splits in the (006)/(102) and (018)/(110) peaks until $z = 0.2$, which indicates the formation of a well-developed layered structure. Meanwhile, those peaks were merged into one and were hard to distinguish for $z = 0.5$ in Fig. 1f. Also, with increasing fluorine content, z, a small impurity peak was observed at around 31° in 2θ in Fig. 1e and f. The XRD patterns clearly indicate that incorporation of F did not alter the crystal structure of $Li[Ni_{1/3}Co_{1/3}Mn_{1/3}]O_2$ nor produce any secondary phases in the range of $z = 0 - 0.15$. By the combination of atomic absorption and ion chromatography (IC) analyses for fluorine, the detected F amounts were 0.05, 0.09, and 0.14 for $z = 0.05$, 0.1, and 0.15, respectively.

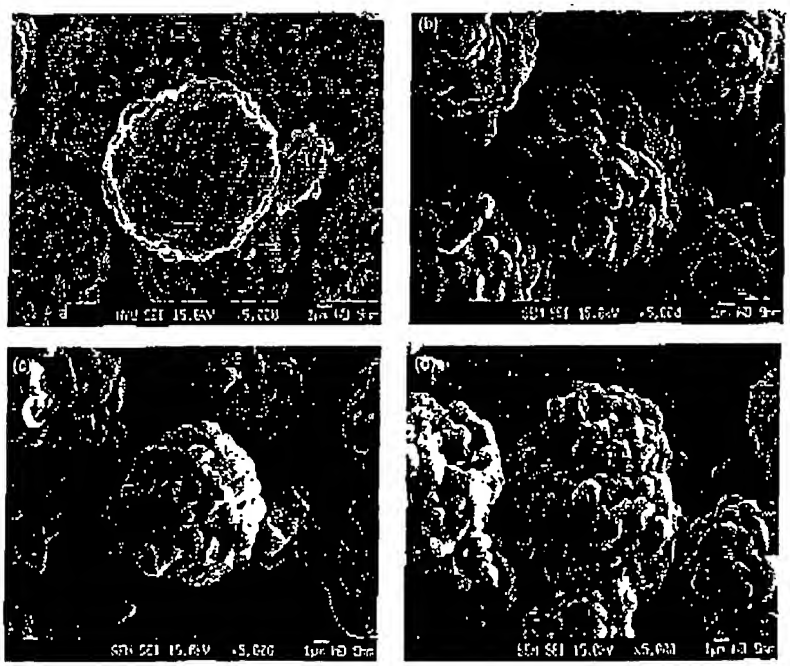

Figure 3. SEM images of $Li[Ni_{1/3}Co_{1/3}Mn_{1/3}]O_{2-z}F_z$: (a) $z = 0$, (b) $z = 0.05$, (c) $z = 0.1$, and (d) $z = 0.15$.

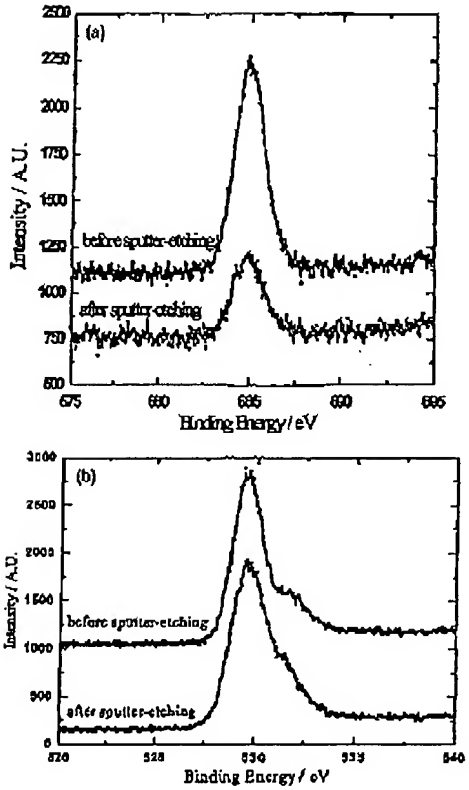

Figure 4. (a) F 1s spectra of $Li[Ni_{1/3}Co_{1/3}Mn_{1/3}]O_{1.95}F_{0.05}$ before and after sputtering with argon ion for 30 min. (b) O 1s spectra of $Li[Ni_{1/3}Co_{1/3}Mn_{1/3}]O_{1.95}F_{0.05}$ before and after sputtering with argon ion for 30 min.

Lattice parameters of the $Li[Ni_{1/3}Co_{1/3}Mn_{1/3}]O_{2-z}F_z$ ($z = 0$, 0.05, 0.1, 0.15, and 0.2) were calculated from the XRD data by a least squares method. Figure 2 shows the variation of the lattice parameters with increasing fluorine content, z. Substitution of fluorine resulted in the increase of the lattice constants in the a axis. During delithiation, the c axis was found to gradually increase, go through a maximum at $z = 0.1$, and then decrease with increasing the fluorine content. The increase in the a axis could be due to the partial reduction of transition metal ions for the charge compensation of F anion. Because the a parameter is a measure of the average M–M (M = Li, Ni, Co, and Mn) distance in the basal plane of the hexagonal structure, the increase in a axis with increasing fluorine content could be attributed to larger Mn^{3+} (0.645 Å) than Mn^{4+} (0.53 Å) or larger Co^{2+} (0.65 Å) than Co^{3+} (0.545 Å).[21] The increase in the c axis also reflects an increase of the ionic radii of partially reduced transition metal ions, which overrode the effect of the slightly smaller F^- (1.33 Å) than O^{2-} (1.40 Å).[21] Increasing fluorine contents of more than 0.1, however, resulted in the decrease of c axis due to the small ionic radius of F anion. XRD results clearly confirm that fluorine ions are successfully substituted for oxygen ions in $Li[Ni_{1/3}Co_{1/3}Mn_{1/3}]O_2$ structure.

Morphology of $Li[Ni_{1/3}Co_{1/3}Mn_{1/3}]O_{2-z}F_z$.—Figure 3 shows the SEM images of the $Li[Ni_{1/3}Co_{1/3}Mn_{1/3}]O_{2-z}F_z$ ($z = 0$, 0.05, 0.1, and 0.15) powders. All powders consist of sphere-shaped particles with average diameter of ~10 μm. Each sphere-shaped particle also consists of agglomerates of smaller primary particles. $Li[Ni_{1/3}Co_{1/3}Mn_{1/3}]O_2$ has the primary particles with average diameter of ~1 μm having round edges in Fig. 3a. When fluorine content increased, primary particles grew up and their shapes gradually changed from round-edged to well-developed polygonal forms. In fact, all the primary particles in $Li[Ni_{1/3}Co_{1/3}Mn_{1/3}]O_{0.85}F_{0.15}$ have well-developed facets in Fig. 3d. It is notable that similar morphological variation is prominent in anion-doped spinels.[22] When fluorine or sulfur was substituted for O in $LiMn_2O_4$, the primary particles changed to well-developed octahedrons with the growth in the particle size. Morphological changes depending on the fluorine content suggest that fluorine substitution not only effects the bulk structures but alters the surface energy of the resulting powders, which accordingly leads to the changes in growth kinetics and final morphology of the powders.

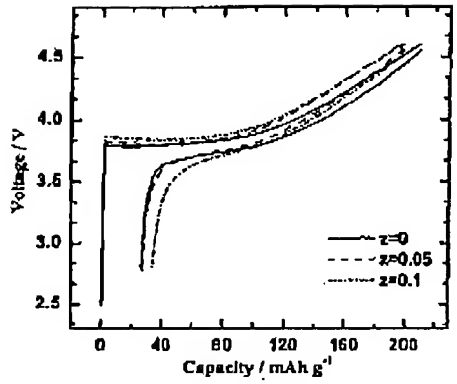

Figure 5. Initial charge and discharge curves of $Li/Li[Ni_{1/3}Co_{1/3}Mn_{1/3}]O_{2-z}F_z$ ($z = 0$–0.15) cells at a current density of 28 mA g^{-1} (0.2 C rate) at 30°C.

XPS analysis of $Li[Ni_{1/3}Co_{1/3}Mn_{1/3}]O_{2-z}F_z$.—In order to study the distribution of fluorine within a particle, X-ray photoelectron spectroscopy (XPS) analysis of $Li[Ni_{1/3}Co_{1/3}Mn_{1/3}]O_{1.95}F_{0.05}$ was carried out. F 1s and O 1s spectra were obtained from the sample before and after sputter-etching the particle surface and are shown in Fig. 4. The binding energy for F 1s measured from Fig. 4a was 684.9 eV, which closely matches those of metal fluorides. In LiF, MnF_2, and NiF_2, the binding energy for F 1s lies between 648.5 and 685.9 eV;[23-25] hence, the fluorine in the compound exists as F^{-1}. When the surface of the powder was sputter-etched using an Ar ion beam for 30 min at an approximate rate of 1 Å/min, the intensity of the F 1s peak was nearly halved after etching away the surface, which suggests that the majority of the F ions reside near the surface of the particle. When the O 1s peaks were examined before and after sputter-etching the surface, the O 1s intensity did not decrease as seen in Fig. 4b, in contrast to the F 1s peaks. Although the relative intensity of the O 1s peak remained unchanged, there was a noticeable change in the peak shape before and after etching. Prior to sputtering, the O 1s spectrum contained a distinct shoulder near 532 eV. After the top surface was etched away, however, the rising of intensity near 531 eV made it hard to distinguish the shoulder. The binding energy of O 1s for most of the Co, Ni, and Mn oxides falls between 529 and 531 eV, in agreement with the main peak of O 1s spectra in Fig. 4b.[26,27] Although the analogous binding energies of Co, Ni, and Mn oxides hinder calculation of their separated values, the increased intensity of the shoulder peak in Fig. 4b may indicate a change in the oxidation state of transition metals in response to the increased concentration of fluorine near the surface. Although detailed investigation is needed to substantiate this, XRD

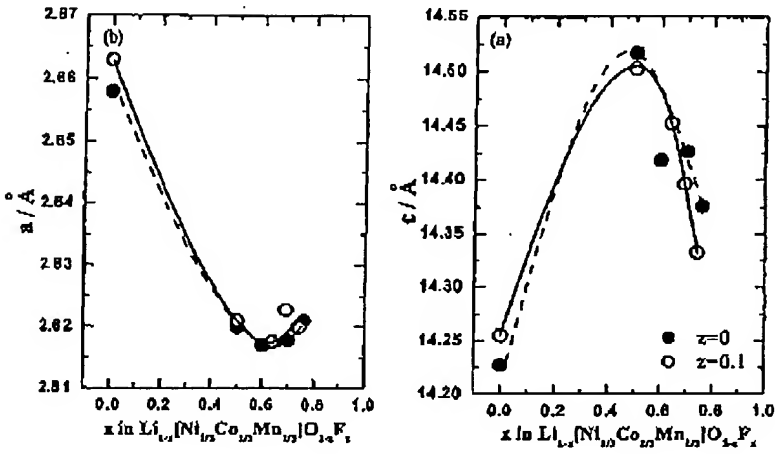

Figure 6. Variation of lattice parameters of $Li[Ni_{1/3}Co_{1/3}Mn_{1/3}]O_{2-z}F_z$ ($z = 0$ and 0.1) electrodes during delithiation: (a) c axis and (b) a axis.

and XPS analysis clearly demonstrated that fluorine resides in the bulk as well as near the surface of the particle, accompanied by possible changes in the oxidation state of the transition metal components.

Electrochemical behavior of $Li[Ni_{1/3}Co_{1/3}Mn_{1/3}]O_{2-z}F_z$.—Figure 5 shows the initial voltage vs capacity profiles of $Li/Li[Ni_{1/3}Co_{1/3}Mn_{1/3}]O_{2-z}F_z$ cells ($x = 0 - 0.1$). At the first cycle, the cells were slowly charged and discharged between 2.8 and 4.6 V with a current density of 28 mA g^{-1} (0.2 C rate) at 30°C. The initial discharge capacity of the $Li/Li[Ni_{1/3}Co_{1/3}Mn_{1/3}]O_{2-z}F_z$ cells decreased as the fluorine content increased; their values were 182 mAh g^{-1} ($z = 0$), 170 mAh g^{-1} ($z = 0.05$), and 165 mAh g^{-1} ($z = 0.1$), respectively. It is likely that a stronger Li–F bond (577 kJ mol^{-1}) than Li–O (341 kJ mol^{-1}) would hinder intercalation of Li^+ ions, which in turn lowers discharge capacities.[21]

On charging, variation of lattice parameters was observed in the range of 2.8–4.6 V for the $Li_{1-x}[Ni_{1/3}Co_{1/3}Mn_{1/3}]O_{2-z}F_z$ ($z = 0$ and 0.1) electrodes in Fig. 6. In layered cathode materials, the c axis first elongates during Li^+ extraction due to the generation of coulombic repulsions between the MO_2 (M = transition metals) layers as the lithium ions which screen the oxygen-oxygen repulsions are removed. In Fig. 6a, both electrodes showed increase in c axis at first, which maximized at $x \approx 0.5$ and then decreased again. Interestingly, the fluorine-doped sample showed less elongation in the c axis than did the fluorine-free sample at $x = 0.5$. From this result, it can be speculated that electrostatic repulsion between oxide ions is partially offset by strong Li–F bonding during Li^+ extraction. Both samples exhibited similar values of a parameters on charging.

Figure 7 shows the differential capacity (dQ/dV) vs voltage profiles of $Li/Li[Ni_{1/3}Co_{1/3}Mn_{1/3}]O_{2-z}F_z$ ($z = 0$, 0.05, and 0.1) cells during 50 cycles. The cells were cycled between 2.8 and 4.6 V with a current density of 28 mA g^{-1}. At the first cycle, the $Li/Li[Ni_{1/3}Co_{1/3}Mn_{1/3}]O_2$ cell exhibited redox peaks at around 3.75 V on charging and 3.74 V on discharging. As the cycling proceeded, however, the redox peaks became more polarized and then shifted to 3.8 and 3.67 V at the 50th cycle. In addition, decrease of initial discharge voltage (indicated with arrow) suggests the increase of internal resistance (IR) during cycling. Together with the increasing polarization between redox peaks, the voltage drop due to IR implies increasing cell resistance during cycling in the $Li/Li[Ni_{1/3}Co_{1/3}Mn_{1/3}]O_2$ cell. This redox voltage variation, however, reduced for $z = 0.05$ and was finally negligible for $z = 0.1$. Identical dQ/dV curves of the fluorine-substituted sample shows its stable redox reaction during cycling compared to the undoped one.

Figure 8 shows the variation of discharge capacities of the $Li/Li[Ni_{1/3}Co_{1/3}Mn_{1/3}]O_{2-z}F_z$ ($z = 0$–0.1) cells during cycling in the range of 2.8–4.6 V. Although the $Li/Li[Ni_{1/3}Co_{1/3}Mn_{1/3}]O_2$ samples had the highest discharge capacity at first, they showed abrupt decrease in capacity during cycling and exhibited 87% of capacity retention at the 50th cycle. The poor capacity retention of $Li/Li[Ni_{1/3}Co_{1/3}Mn_{1/3}]O_2$ is primarily due to its high voltage cutoff, because it exhibited good capacity retention with the capacity of 155 mAh g^{-1} in the range of 2.8–4.3 V. Meanwhile, though fluorine-substituted samples had lower initial capacities, they showed far better capacity retentions during 50 cycles in the same voltage range, 96% for $z = 0.05$ and 97% for $z = 0.1$ at the 50th cycle, respectively.

In order to observe long-term cycling properties, a carbon electrode was employed as the negative electrode. Figure 9 exhibits discharge capacity vs. cycle number for $C/Li[Ni_{1/3}Co_{1/3}Mn_{1/3}]O_2$ and $C/Li[Ni_{1/3}Co_{1/3}Mn_{1/3}]O_{1.95}F_{0.05}$ cells by applying 1 C (140 mA g^{-1}) between 2.8 and 4.5 V. The $C/Li[Ni_{1/3}Co_{1/3}Mn_{1/3}]O_2$ delivered somewhat higher capacity in the early stage of cycling compared to $C/Li[Ni_{1/3}Co_{1/3}Mn_{1/3}]O_{1.95}F_{0.05}$. However, the higher capacity faded gradually as the cycling continued. The capacity retention was about 75% at the 100th cycle. On the contrary, though $C/Li[Ni_{1/3}Co_{1/3}Mn_{1/3}]O_{1.95}F_{0.05}$ exhibited slightly smaller capacity, the capacity was greatly retained and capacity retention was about 94% of its initial discharge capacity at the 100th cycle in Fig. 9.

Although more experimental works are required for clear explanation about the poor electrochemical properties of $Li[Ni_{1/3}Co_{1/3}Mn_{1/3}]O_2$ at high-voltage cutoff in detail, previous works reported the possible Co dissolution during cycling. Amatucci et al.[6] reported that the amount of Co dissolution became significant in $LiCoO_2$ when voltage cutoff was higher than 4.2 V. Furthermore, fluorine coating effectively reduced the dissolution of particles into electrolyte by passivation of particles.[19] From the viewpoint of Co dissolution, we could explain why the capacity of $Li[Ni_{1/3}Co_{1/3}Mn_{1/3}]O_2$ was deteriorated when the voltage cutoff was higher than 4.4 V, especially at 4.6 V. Hence, it is likely that the fluorine coating on the surface of $Li[Ni_{1/3}Co_{1/3}Mn_{1/3}]O_{2-z}F_z$ protects the active material from HF attack into electrolyte and makes it possible to endure high voltage cutoff.

Rate capability testing also demonstrated the advantages of fluorine substitution. Figure 10 shows voltage profiles of $Li/Li[Ni_{1/3}Co_{1/3}Mn_{1/3}]O_{2-z}F_z$ cells at various C-rates in the range of 0.2–5. As observed in Fig. 10a, the discharge capacity of undoped

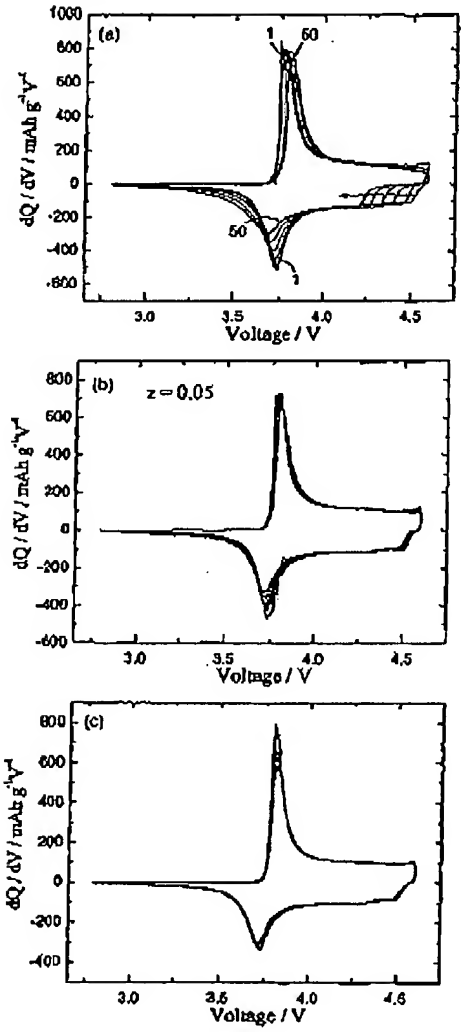

Figure 7. *DQ/dV* curves of $Li/Li[Ni_{1/3}Co_{1/3}Mn_{1/3}]O_{2-z}F_z$ ($z = 0$–0.1) cells during 50 cycles at a current density of 28 mAg^{-1} (0.2 C rate) at 30°C.

$Li/Li[Ni_{1/3}Co_{1/3}Mn_{1/3}]O_2$ dropped dramatically with increasing C-rate. Moreover, $Li/Li[Ni_{1/3}Co_{1/3}Mn_{1/3}]O_2$ had a large IR and in turn showed low operating voltages at high C-rates. However, a small amount of fluorine substitution gave rise to a noticeable improvement in discharge capacity as well as IR drop at the high C-rates in Fig. 10b and c. Together with the effect of fluorine on the Co dissolution, the small variation of c axis in Fig. 6a could explain the superior rate capability of the fluorine-doped sample, because small c axis variation during cycling is advantageous to maintain structural stability, especially at high rates. $Li/Li[Ni_{1/3}Co_{1/3}Mn_{1/3}]O_{1.9}F_{0.1}$ exhibited the best rate capability in Fig. 10c, showing 70% capacity retention at 5 C rate compared to its capacity at 0.2 C.

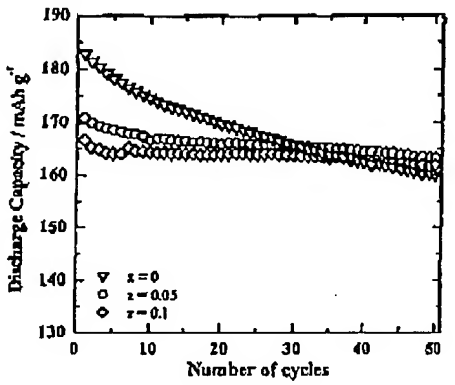

Figure 8. Cycling performance of $Li/Li[Ni_{1/3}Co_{1/3}Mn_{1/3}]O_{2-z}F_z$ ($z = 0$–0.1) cells during 50 cycles at a current density of 28 mA g^{-1} (0.2 C rate) at 30°C.

Volumetric capacity of $Li[Ni_{1/3}Co_{1/3}Mn_{1/3}]O_{2-z}F_z$.—For practical applications, PD of positive material is an important point with regard to volumetric capacity. Cathode material with high PD could provide high volumetric capacity within a limited inner space of practical battery. As the fluorine content increased, tap density also increased from 2.9 g cm^{-3} ($z = 0$) to 3.21 g cm^{-3} ($z = 0.05$ and 0.1) because of growing primary particles in Fig. 3.

Specific gravimetric and volumetric capacities of the $Li[Ni_{1/3}Co_{1/3}Mn_{1/3}]O_{2-z}F_z$ ($z = 0$, 0.05, and 0.1) powders were compared in Fig. 11. Each capacity was measured at a 0.2 C rate. Although fluorine-doped samples had low gravimetric capacities, they exhibited high volumetric capacities compared to $Li[Ni_{1/3}Co_{1/3}Mn_{1/3}]O_2$ because of their high PD. Among them, $Li[Ni_{1/3}Co_{1/3}Mn_{1/3}]O_{1.95}F_{0.05}$ exhibited the highest volumetric capacity of 547 mAh cm^{-3}, while $Li[Ni_{1/3}Co_{1/3}Mn_{1/3}]O_2$ showed

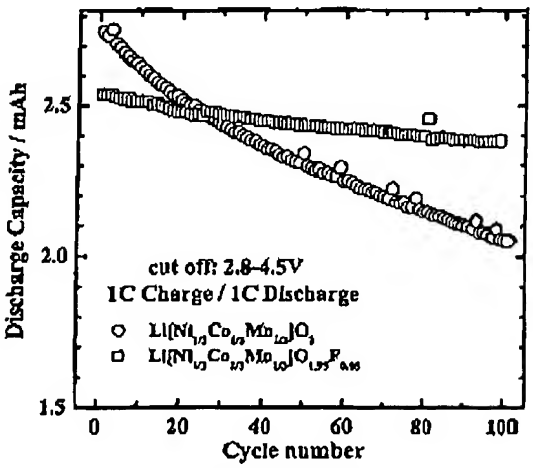

Figure 9. Discharge capacity vs cycle number of $C/Li[Ni_{1/3}Co_{1/3}Mn_{1/3}]O_2$ and $C/Li[Ni_{1/3}Co_{1/3}Mn_{1/3}]O_{1.95}F_{0.05}$ cells during 100 cycles by applying a current density of 1 C (140 mA g^{-1}) at 30°C.

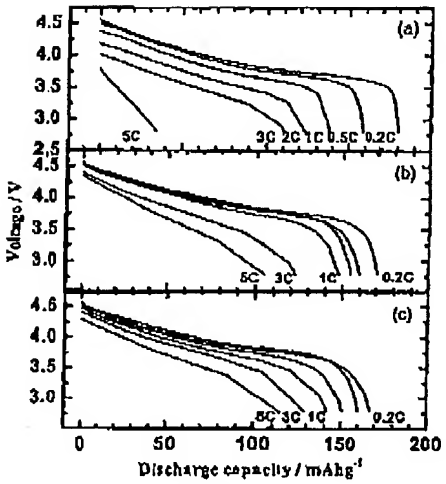

Figure 10. Rate capability of Li/Li[$Ni_{1/3}Co_{1/3}Mn_{1/3}$]$O_{2-z}F_z$ (z = 0–0.1) cells at 30°C: (a) z = 0, (b) z = 0.05, and (c) z = 0.1.

531 mAh cm^{-3}. This result confirms that slightly low gravimetric capacities of fluorine-doped samples could be offset by their high volumetric capacities.

Thermal stability of Li[$Ni_{1/3}Co_{1/3}Mn_{1/3}$]$O_{2-z}F_z$.—Thermal stability of positive materials, especially at delithiated state, is an important factor in judging the suitability for practical application of lithium secondary batteries. Figure 12 shows DSC profiles of wet electrodes of Li_{1-x}[$Ni_{1/3}Co_{1/3}Mn_{1/3}$]$O_{2-z}F_z$ which were charged to 4.6 V. The DSC experiments were made in welded sealed stainless steel tubes so that no leaking of pressurized electrolyte was possible. As the concentration of fluorine in Li_{1-x}[$Ni_{1/3}Co_{1/3}Mn_{1/3}$]$O_{2-z}F_z$ increased, the thermal stability of the charged cathode material in the electrolyte was greatly improved. The Li_{1-x}[$Ni_{1/3}Co_{1/3}Mn_{1/3}$]O_2 had a large exothermic peak between 234 and 283°C which produced 4227 J g^{-1} of heat. When fluorine content increased, Li_{1-x}[$Ni_{1/3}Co_{1/3}Mn_{1/3}$]$O_{2-z}F_z$ showed higher onset temperature of exothermic peak and lower heat amount; 280°C with 1733 J g^{-1} for

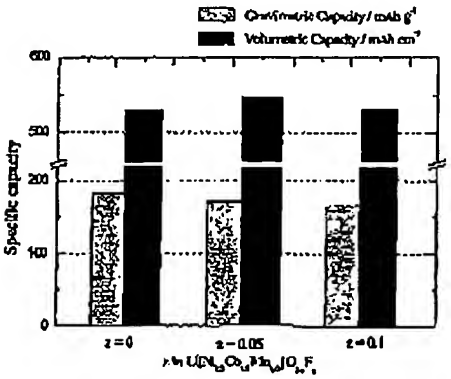

Figure 11. Comparison of gravimetric and volumetric discharge capacities of Li/Li[$Ni_{1/3}Co_{1/3}Mn_{1/3}$]$O_{2-z}F_z$ (z = 0–0.1) cells at a current density of 28 mA g^{-1} (0.2 C rate) at 30°C.

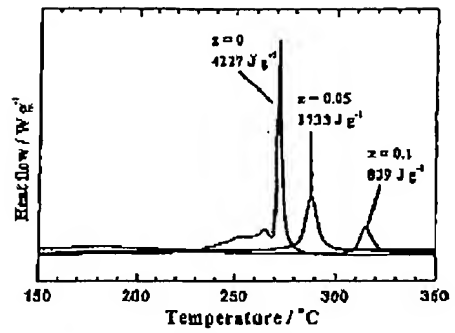

Figure 12. Comparison of DSC traces of Li_{1-x}[$Ni_{1/3}Co_{1/3}Mn_{1/3}$]$O_{2-z}F_z$ (z = 0–0.1) at 4.6 V.

z = 0.05 and 308°C with 839 J g^{-1} for z = 0.1, respectively. Improved thermal stability of fluorine-doped samples shows the structural stability of Li_{1-x}[$Ni_{1/3}Co_{1/3}Mn_{1/3}$]$O_{2-z}F_z$ at highly charged state of 4.6 V.

Conclusion

In this paper we report the structure, morphology, electrochemical properties, and thermal stability of Li[$Ni_{1/3}Co_{1/3}Mn_{1/3}$]$O_{2-z}F_z$. Variation of lattice parameters according to fluorine content, z, suggests that fluorine is partly substituted in bulk structure. XPS analysis also shows that the majority of the fluorine ions reside near the surface of the particle. These results suggest that fluorine ions are both in bulk and on the surface of Li[$Ni_{1/3}Co_{1/3}Mn_{1/3}$]$O_{2-z}F_z$. Fluorine substitution catalyzes the growth of the primary particles as confirmed by SEM, which in turn results in high tap density as well as high volumetric capacity compared to Li[$Ni_{1/3}Co_{1/3}Mn_{1/3}$]O_2.

Although capacity fading was observed for Li[$Ni_{1/3}Co_{1/3}Mn_{1/3}$]O_2 at high voltage cutoff of 4.6 V, Li[$Ni_{1/3}Co_{1/3}Mn_{1/3}$]$O_{2-z}F_z$ shows good capacity retention. In addition, Li[$Ni_{1/3}Co_{1/3}Mn_{1/3}$]$O_{2-z}F_z$ exhibits superior rate capability compared to an F-free sample, probably due to the smaller c axis variation and fluorine coating effects. DSC measurement at 4.6 V clearly shows that fluorine substitution markedly improves the thermal stability of Li[$Ni_{1/3}Co_{1/3}Mn_{1/3}$]$O_{2-z}F_z$.

Acknowledgment

This work was performed through the financial support of the National R&D programs of the Ministry of Science and Technology, Republic of Korea.

Hanyang University assisted in meeting the publication costs of this article.

References

1. D. D. MacNeil, Z. Lu, and J. R. Dahn, *J. Electrochem. Soc.*, 149, A1332 (2002).
2. T. Ohzuku and Y. Makimura, *Chem. Lett.*, 30, 642 (2001).
3. S.-H. Kang, J. Kim, M. E. Stoll, D. Abraham, Y. K. Sun, and K. Amine, *J. Power Sources*, 112, 41 (2002).
4. K. M. Shaju, G. V. Subba Rao, and B. V. R. Chowdari, *Electrochim. Acta*, 48, 145 (2002).
5. G.-H. Kim, S.-T. Myung, H. J. Bang, J. Prakash, and Y.-K. Sun, *Electrochem. Solid-State Lett.*, 7, A477 (2004).
6. G. G. Amatucci, J. M. Tarascon, and L. C. Klein, *Solid State Ionics*, 83, 167 (1996).
7. H. Tukamoto and A. R. West, *J. Electrochem. Soc.*, 144, 3164 (1997).
8. Y.-I. Jang, B. Huang, H. Wang, D. R. Sadoway, G. Ceder, Y.-M. Chiang, H. Liu, and H. Tamura, *J. Electrochem. Soc.*, 146, 862 (1999).
9. M. Mladenov, R. S. Stoyanova, E. Zhecheva, and S. Vassilev, *Electrochem. Commun.*, 3, 410 (2001).
10. H. Wang, Y.-I. Jang, B. Huang, D. R. Sadoway, and Y.-M. Chiang, *J. Power Sources*, 81–82, 594 (1999).
11. G. Ceder, Y.-M. Chiang, D. R. Sadoway, M. K. Aydinol, Y.-I. Jang, and B. Huang,

Nature (London), 392, 694 (1998).
12. S.-T. Myung, N. Kumagai, S. Komaba, and H.-T. Chung, *Solid State Ionics*, 139, 47 (2001).
13. J. Cho, Y. J. Kim, and B. Park, *Chem. Mater.*, 12, 3788 (2000).
14. Z. Chen and J. R. Dahn, *Electrochem. Solid-State Lett.*, 5, A213 (2002).
15. M. C. Fredel and A. R. Boccaccini, *J. Mater. Sci.*, 39, 4373 (1996).
16. A. M. Kannan, L. Rabenberg, and A. Manthiram, *Electrochem. Solid-State Lett.*, 6, A16 (2003).
17. Z. Chen and J. R. Dahn, *Electrochem. Solid-State Lett.*, 5, A213 (2002).
18. T. Ohzuku, A. Ueda, and M. Kouguchi, *J. Electrochem. Soc.*, 142, 4033 (1995).
19. Y. Fumihiro, O. Hirokuni, and Y. Nobuyuki, Jpn. Pat. 2003-221215 (2003.08.05).
20. M.-H. Lee, Y.-J. Kang, S.-T. Myung, and Y.-K. Sun, *Electrochim. Acta*, 50, 939 (2004).
21. J. A. Dean, *Lange's Handbook of Chemistry*, 15th ed., pp. 9.3.1–4.5.3, McGraw-Hill, New York (1999).
22. S.-H. Park, K.-S. Park, Y.-K. Sun, and K.-S. Nahm, *J. Electrochem. Soc.*, 147, 2116 (2000).
23. G. E. Murch and R. J. Thorn, *J. Phys. Chem. Solids*, 48, 785 (1980).
24. A. Aoki, *Jpn. J. Appl. Phys.*, 15, 305 (1976).
25. B. P. Loechel and H. H. Strehblow, *J. Electrochem. Soc.*, 131, 713 (1984).
26. J. Haber, J. Stoch, and L. Ungier, *J. Electron Spectrosc. Relat. Phenom.*, 9, 459 (1976).
27. M. Oku, K. Hirokawa, and S. Ikeda, *J. Electron Spectrosc. Relat. Phenom.*, 7, 465 (1975).